Time-resolved spectroscopic imaging reveals the fundamentals of cellular NADH fluorescence

Dong Li, Wei Zheng, and Jianan Y. Qu*

Department of Electronic and Computer Engineering, Hong Kong University of Science and Technology, Clear Water Bay, Kowloon, Hong Kong, China
**Corresponding author: eequ@ust.hk*

Received June 27, 2008; revised August 19, 2008; accepted August 26, 2008;
posted September 11, 2008 (Doc. ID 98033); published October 14, 2008

A time-resolved spectroscopic imaging system is built to study the fluorescence characteristics of nicotinamide adenine dinucleotide (NADH), an important metabolic coenzyme and endogenous fluorophore in cells. The system provides a unique approach to measure fluorescence signals in different cellular organelles and cytoplasm. The ratios of free over protein-bound NADH signals in cytosol and nucleus are slightly higher than those in mitochondria. The mitochondrial fluorescence contributes about 70% of overall cellular fluorescence and is not a completely dominant signal. Furthermore, NADH signals in mitochondria, cytosol, and the nucleus respond to the changes of cellular activity differently, suggesting that cytosolic and nuclear fluorescence may complicate the well-known relationship between mitochondrial fluorescence and cellular metabolism. © 2008 Optical Society of America

OCIS codes: 170.6920, 300.6500, 170.1530.

Nicotinamide adenine dinucleotide (NADH) is a well-known metabolic coenzyme playing important roles in a variety of cellular metabolic pathways. In mitochondria, NADH is a major electron donor in the electron transport chain and a product of the citric-acid cycle [1]. In cytosolic energy metabolism, NAD+ and NADH mediate glycolysis via the oxidation of glyceraldehyde 3-phosphate to 1,3-bisphosphoglycerate and the lactate–pyruvate conversions catalyzed by lactate dehydrogenase [1]. Furthermore, NADH is also involved in many pathways not directly related to cellular metabolism. For instance, increased evidence suggests that NADH regulates certain corepressors, such as CtBP, to bind with its partners in the nucleus. This influences the transcriptional pathways that are important for cell development and cycle regulation [2,3].

Though NADH functions differently in different cellular activity pathways, previous studies focused mainly on the measurements and interpretations of NADH fluorescence emitted from mitochondria, because it is a major source of NADH signal in cell or tissue [4,5]. Recently, we demonstrated that the time-resolved autofluorescence spectroscopy could distinguish free NADH fluorescence from protein-bound NADH fluorescence, and the ratio of NADH in free form over the protein-bound form is a sensitive indicator of cellular energy metabolism [6]. In this Letter, we extend our study to analyze NADH signals in different cellular organelles using time-resolved spectroscopic imaging. We analyze NADH signals measured from three major cellular compartments: the mitochondria, the nucleus, and the cytosol. For the first time to our knowledge, we demonstrate that NADH exists in free and protein-bound form in these compartments and that the changes of NADH fluorescence in these components are associated with different cellular activities.

The time-resolved spectroscopic imaging system was modified from the previously reported fluorescence lifetime spectroscopy system [6]. Briefly, a femtosecond Ti:sappphire laser and its second-harmonic generation were used as the excitation sources for two-photon excited fluorescence (TPF) and single-photon excited fluorescence (SPF), respectively. A water immersion objective lens (60×, 1.20 NA) was used to focus the excitation beam into the sample and collect the backscattered fluorescence signals. The depth scanning was controlled by an actuator. A pair of galvo mirrors scanned the beam laterally and created a 60×60 μm sampling area in the examined sample. When the system was set to measure the SPF signal, a dichroic mirror and a long-pass filter with the same cut-off wavelength at 400 nm were used to separate the SPF signal from the excitation light. A tube lens with 400 mm effective focal length focused the fluorescence into a 100 μm core optical fiber that worked as a pinhole to collect the confocal SPF signal and to conduct the signal to the spectrograph. A dichroic mirror of the cut-off wavelength at 650 nm and a shortpass filter of cut-on wavelength at 700 nm were used when measuring TPF signals. A 80 mm tube lens and 400 μm core optical fiber were used to effectively collect the TPF signals and to conduct the signals to the spectrograph. The spectrograph was equipped with a multichannel photo multiplier tube (PMT) and a time-correlated single photon counting module (PML-16 and SPC-150, Becker & Hickl GmbH) to measure the time- and spectral-resolved SPF or TPF signals from each pixel of the imaged sample. The SPF and the TPF were recorded in the wavelength range from 400 to 600 nm with ~13 nm resolution. The advantage of this system is to measure SPF and TPF signals from the same sample. The information on NADH extracted from SPF and TPF signals measured in different cellular components provides cross verification.

The samples used in this study were the monolayer cultured SiHa cells. To ensure NADH fluorescence as

0146-9592/08/202365-3/$15.00 © 2008 Optical Society of America

the dominant signal in the autofluorescence of a sample, the excitation wavelengths for SPF and TPF measurements were set at 365 and 730 nm, respectively [4,6]. To reduce photobleaching, the excitation powers on samples were kept about 5 μW and 8 mW for SPF and TPF measurements, respectively. The acquisition time for an image of 128×128 pixels over 60×60 μm sampling area is about 128 s. Fluorescence beads of 0.2 μm in diameter were used to measure the system resolution. The systems in the SPF confocal and TPF imaging configurations produced almost-identical lateral and axial resolutions of about 0.45 and 1.8 μm, respectively. Typical SPF and TPF images of SiHa cell culture samples are presented in Fig. 1. The gamma of all images is set to 0.5 for better display of three cellular compartments: mitochondria, cytosol, and nucleus. The gray level is presented in pseudocolor. As can be seen from the SPF and TPF images, the fluorescence intensity of mitochondria, the bright spots and stripes presented from cyan to red, are much higher than the fluorescence from cytosol and nucleus, presented mainly in blue. In this study, we found that the information extracted from SPF and TPF images and signals are equivalent. The analyses of SPF signals are therefore used as representative results in the following discussions.

The signal quality of each pixel in the image was not sufficiently high to obtain reliable temporal and spectral characteristics of the fluorescence signal, because the highest intensity of a pixel was about 150 counts in a single PMT channel. For accurate analysis of the autofluorescence signals, we divided the image of a cell into three compartments of mitochondria, cytosol, and nucleus. The pixel signals in the three compartments were summed up into high-quality summed-up signals of mitochondria, cytosol, and nucleus. The summed-up signals were used in the analyses of the fluorescence spectra and lifetimes. Technically, we used threshhold based edge detection to localize the mitochondria with significantly higher photon counts and define the boundary between nucleus and cytosol. The representative results are shown in Fig. 2. The images of three compartments measured from Fig. 2(a) are shown in Figs. 2(b)–2(d). The locations and areas of mitochondria and nucleus were verified by using the fluorescence-labeling method. The measurements based on the results in Fig. 2 show that the proportional contributions of mitochondria, cytosol, and nucleus to total fluorescence of the cell section are about 70%, 20%, and 10%, respectively. Typical counts of mitochondria, cytosol, and nucleus compartments in the PMT channel at 450 nm are about 6×10^4, 2×10^4, and 1×10^4, respectively, which are sufficient for accurate fitting analyses.

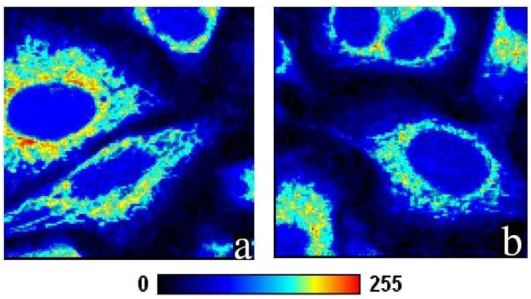

Fig. 1. (Color online) Representative images of SiHa cell culture in pseudocolor: (a) SPF image; (b) TPF image.

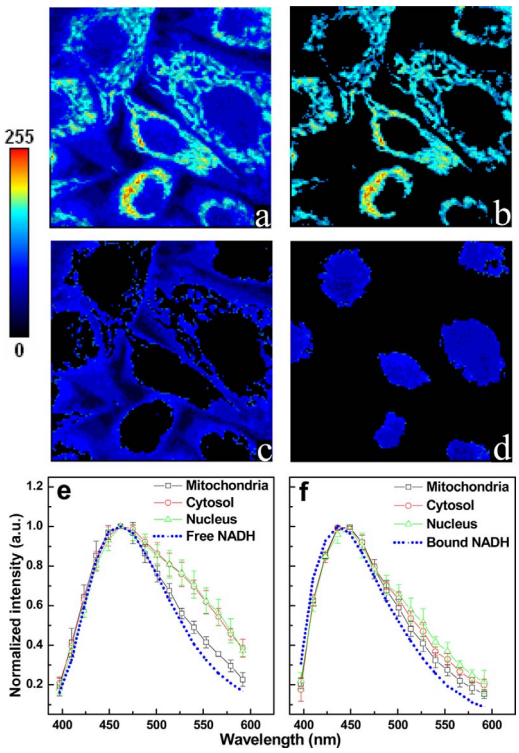

Fig. 2. (Color online) Pseudocolor images and decay associate spectra (DAS) signals of three cellular compartments: (a) SPF image of SiHa cells; (b) extracted mitochondrial compartment; (c) cytosolic compartment; (d) nuclear compartment; (e) normalized short lifetime DAS of SiHa cells and fluorescence spectrum of pure NADH; (f) Normalized long lifetime DAS of SiHa cells and fluorescence spectrum of NADH bound with lactate dehydrogenase (LDH).

A dual exponential decay model, $A_1\exp(-t/\tau_1)+A_2\exp(-t/\tau_2)$, was used in the fitting analyses of the summed-up fluorescence signals, where τ_1 and τ_2 are the time-decay constants, respectively, and A_1 and A_2 are the amplitudes of two decay terms, respectively. The calculated DAS of mitochondria, cytosol, and nucleus are shown in Figs. 2(d) and 2(f), respectively. As can be seen, the short- and long-lifetime DAS of three components peak at around 460 and 440 nm, respectively. The comparison between short-lifetime DAS and free NADH spectrum demonstrates that the free NADH signal is dominant in the short-lifetime decay term, while the blueshift of long-lifetime DAS is consistent with that of NADH bound with LDH, one of enzymes in cellular metabolic pathways [1,6]. Though the mitochondrial DAS signals are close to the free and bound NADH spectra, there are obvious shoulders in the DAS signals of cytosol and nucleus in the long-wavelength region. Previous studies have shown that the fluorescence of cytokeratins and lipopigments are peaked in the 500–600 nm region, suggesting that the spectral shoulders may be originated from cytokeratins or lipopigmnets [7,8].

Table 1. A_1/A_2 Ratio and Lifetimes Measured from SiHa Cell Cultures[a–c]

Treatment		Control	NaCN	D-glucose	Cd
M	A_1/A_2	5.5	7.6	5.3	7.4
	τ_1 (ns)	0.37	0.36	0.38	0.37
	τ_2 (ns)	3.24	3.21	3.31	3.27
C	A_1/A_2	6.6	6.7	5.8	10.5
	τ_1 (ns)	0.36	0.37	0.39	0.34
	τ_2 (ns)	3.05	2.99	3.39	2.91
N	A_1/A_2	8.2	8.0	6.5	13.5
	τ_1 (ns)	0.36	0.36	0.37	0.33
	τ_2 (ns)	2.89	2.95	3.08	2.73

[a] *M*, mitochondria; *C*, cytosol; *N*, nucleus.

[b] Ratios and lifetimes are calculated based on the short- and long-lifetime DAS in the wavelength band 430–460 nm, where free and bound NADH fluorescence are peaked.

[c] The values of all parameters are based on the average over five measurements. Maximal error is 10%.

The fitting parameters calculated from the measurements of cell cultures before and after treated with chemicals are summarized in Table 1. In control samples, the ratio of free to bound NADH in cytosol and nucleus was slightly higher than that in mitochondria, which may indicate a higher viscosity in mitochondrial matrix space. To manipulate the cytosolic metabolism, the SiHa cell cultures were treated with deoxyglucose, an inhibitor of glycolysis in cytosol [9]. As shown in Table 1, the treatment with 20 mM deoxyglucose caused a significant decrease of the A_1/A_2 ratio, reflecting a decrease of the ratio of free-over-bound NADH. This is due to the fact that the deoxyglucose blocks the production of free NADH in cytosol [1,9]. Because free NADH can diffuse through the nuclear pore, the change of free NADH in a nuclear compartment may be associated with the decrease of free NADH in cytosol [3]. However, the A_1/A_2 ratio in mitochondria was almost unchanged, indicating that the deoxyglucose may have little effect on mitochondrial NADH equilibrium.

The NaCN is an inhibitor of the mitochondrial electron transport chain [1], which blocks the NADH oxidation and causes free NADH accumulation in mitochondria. The results in Table 1 demonstrated a significant increase of the A_1/A_2 ratio in mitochondria after the SiHa cell cultures were treated with 5 mM NaCN, while the A_1/A_2 ratio in the cytosol remained unchanged, because the mitochondrial membrane is impermeable to NADH, and cytosolic NADH produced by glycolysis could be oxidated by lactate–pyruvate conversion [10]. The A_1/A_2 ratio in the nucleus remained almost unchanged after the treatment with NaCN.

The results in Table 1 also show that when SiHa cell cultures were treated with 5 μM Cd, the A_1/A_2 ratio in nucleus and cytosol increased over a factor of 1.5. It is known that Cd is a toxic heavy metal. Low-concentration Cd could stimulate cell growth and DNA synthesis, which are normally regulated by the corepressor of gene expression CtBP [2,11]. Increased evidence indicates that free NADH is a determining factor in regulating CtBP activity [3]. Therefore, the effect of Cd on cell growth may play a major role in the dramatic increase of free NADH and the A_1/A_2 ratio in nucleus. The increase of the A_1/A_2 ratio in mitochondria might be caused by Cd binding to macromolecules and dislodging NADH from its normal binding site [12].

Finally, it was found that the fluorescence lifetimes changed to a certain extent after treatment with the chemicals. In particular, the long lifetime (τ_2) of the cytosolic fluorescence from SiHa cells increased from 3.05 to 3.39 ns after application of deoxyglucose. The chemical may induce a change of binding site profile in the pathways with which NADH is engaged. The changes of fluorescence lifetimes may be associated with the change of binding site profile [5,13].

In conclusion, the autofluorescence from mitochondria, cytosol, and nucleus are separated from each other. It is crucial to use the high-quality summed-up signals of mitochondria, cytosol, and nucleus for accurate characterization of the NADH fluorescence in these cellular compartments. Mitochondrial fluorescence is not completely dominant because a certain amount of NADH/NAD(P)H fluorescence is measured from cytosol and nucleus. The free-to-protein-bound NADH ratio responds to the changes of cellular activity in mitochondria, cytosol, and nucleus differently. The ratio could not only serve as an indicator of cellular aerobic and anaerobic metabolism but also gene expression rate in a nucleus.

This work is supported by the Hong Kong Research Grants Council through grant HKUST6408/05M.

References

1. M. K. Campbell, *Biochemistry*, (Saunders College Publishing, 1995).
2. Q. Zhang, D. W. Piston, and R. H. Goodman, Science **295**, 1895 (2002).
3. C. C. Fjeld, W. T. Birdsong, and R. H. Goodman, Proc. Natl. Acad. Sci. U.S.A. **100**, 9202 (2003).
4. S. Huang, A. A. Heikal, and W. W. Webb, Biophys. J. **82**, 2811 (2002).
5. D. K. Bird, L. Yan, K. M. Vrotsos, K. W. Eliceiri, E. M. Vaughan, P. J. Keely, J. G. White, and N. Ramanujam, Cancer Res. **65**, 8766 (2005).
6. Y. Wu, W. Zheng, and J. Y. Qu, Opt. Lett. **31**, 3122 (2006).
7. J. Beuthan, O. Minet, and G. Muller, Ann. N.Y. Acad. Sci. **838**, 150 (1998).
8. A. C. Croce, A. Ferrigno, M. Vairetti, R. Bertone, I. Freitas, and G. Bottiroli, Photochem. Photobiol. Sci. **3**, 920 (2004).
9. S. Barban and H. O. Schulze, J. Biol. Chem. **236**, 1887 (1961).
10. W. Ying, Antioxid. Redox. Sign. **10**, 1 (2008).
11. T. V. Zglinicki, C. Edwall, E. Ostlund, B. Lind, M. Nordberg, N. R. Ringertz, and J. Wroblewski, J. Cell. Sci. **103**, 1073 (1992).
12. M. S. Yang, D. Li, T. Lin, J. J. Zheng, W. Zheng, and J. Y. Qu, Toxicology **247**, 6 (2008).
13. M. C. Skala, K. M. Riching, D. K. Bird, A. Gendron-Fitzpatrick, J. Eichhoff, K. W. Eliceiri, P. J. Keely, and N. Ramanujam, J. Biomed. Opt. **12**, 024014 (2007).